THE UNIVERSITY OF MICHIGAN

COLLEGE OF ENGINEERING

DEPARTMENT OF ELECTRICAL ENGINEERING

Radiation Laboratory

SIMPLIFIED MODELING TECHNIQUES FOR AVIONIC ANTENNA PATTERN SIGNATURES

Interim Technical Report No. 3
15 October 1965 - 15 January 1966

W. DeHart, J. Ferris and R. Wolford

February 1966

7274-3-T = RL-2150

Contract AF 33(615)-2606
Task 435703, Project 4357

Contract Monitor: K. W. Tomlinson AVWE

Contract With: Air Force Avionics Laboratory
Research and Technology Division
Air Force Systems Command
Wright-Patterson Air Force Base, Ohio 45433

Administered through:

OFFICE OF RESEARCH ADMINISTRATION • ANN ARBOR

TABLE OF CONTENTS

ABSTRACT

To further justify the use of simplified modeling, it has been suggested that consideration be given to the use of fly-by tests (employing an instrumented aircraft) to obtain patterns of a typical airborne antenna at the fundamental, spurious and harmonic frequencies. A discussion of two techniques that may be employed to obtain fly-by tests is presented in this report.

Spectrum signature data has been collected on the AN/ARC-27 transmitter employing three measurement systems and a discussion of the results is included. In addition, techniques for obtaining the output impedance of the transmitter have been further considered and a discussion of the problems is included in this report.

I. INTRODUCTION

The present study is divided into three parts, each to be concerned with the determination of the spectrum signature of airborne electronic systems. The three areas being considered during this study are: 1) practical methods for obtaining the desired antenna pattern spectrum signature at a minimum cost, 2) data recording and reduction techniques, and 3) the system aspect of the problem.

To obtain antenna pattern spectrum signatures consideration has been given to the use of simplified models rather than precision models or an instrumented airborne system. An extensive experimental study has been conducted investigating the feasibility of the simplified modeling technique and the results have been very encouraging. To further justify the use of the simplified model, it has been suggested that consideration should be given to the use of fly-by tests (employing an instrumented full-scale aircraft) to obtain full-scale spectrum signature data at the fundamental, spurious and harmonic frequencies to be further compared with the simplified model data.

Techniques for recording spectrum signature data of antennas and for reducing the data to statistical format are also being investigated during this study. Data recording techniques have been centered around the use of digital recording systems so that data can be later reduced into a statistical format to aid in prediction and analysis. A technical report of the data recording and reduction procedures is being prepared.

During the system portion of the study, consideration is being given to methods for determining the output impedance characteristics of the transmitter at the fundamental, spurious and harmonic frequencies. The purpose of this study is to determine a practical method for obtaining the output impedance characteristic of the transmitter so that more accurate interference predictions can be made of airborne systems. A justification for this study is based on the inaccuracies that have been noted in the interference prediction analysis made of airborne systems. Further, the data collected will be more basic in nature and therefore be applicable to a wider range of antenna and transmitter configurations.

II. SIMPLIFIED MODELING

In the second interim* it was noted that the study of simplified modeling was drawing to a conclusion. To insure that all areas pertinent to obtaining airborne antenna spectrum signatures have been properly investigated, further consideration has been given to the use of a full scale aircraft. The full scale aircraft antenna study would necessitate the use of fly-by tests. From these signature data would be obtained for comparison to simplified model data.

2.1 Fly-By Tests

To ensure that adequate fly-by test data would be obtained, a simplified model of the aircraft to be flown during the fly-by tests would be required, and a set (at all frequencies of interest) of three dimensional antenna pattern data collected. Further, it would be necessary for the antenna used on the simplified model to be similar in configuration and location to that used on the full scale model. To carry out the fly-by tests two facilities have been investigated and will be discussed in the following sections of the report.

2.1.1 Fly-By Tests WPAFB

Consideration was at first given to the use of the Trebein facilities at Wright Field. A factor in favor of the use of the Trebein's facilities is a 40 foot parabolic reflector located there. In addition to the dish, several HF receivers and auto-

---

* "Simplified Modeling Techniques for Avionic Antenna Pattern Signatures" Interim Technical Report No. 2, 15 July - 15 October, 1965, W. DeHart J. Ferris and R. Wolford, under Contract AF-33(615)-2606

matic recording systems are available. In addition to these facilities two UHF receiver types would be required similar to those manufactured by the Stoddard and Empire Device Corporations.

The two UHF receivers noted above have an input sensitivity of 10 micro volts in the UHF band which is equivalent to -87 dbm into a 50 ohm load. The gain and pattern characteristics of the 40 foot parabolic reflector are shown in Table I. To obtain an insight into the transmitter power levels that may be associated with an ARC-27 transmitter, the data presented in Table II has been extracted from several reports from the Army Electronic Proving Ground, Fort Huachua, Arizona entitled Spectrum Signature Data of Radio Set AN/ARC-27. The slant range from the airborne antenna to the 40 foot parabolic receiving antenna was calculated from the geometry of the problem shown in Fig. 1. Using the above parameters and the Friis transmission formula, the general expression for the received power may be determined as shown below.

$$P = \frac{P_t G_t A_e}{4 \pi S^2}$$

where

P_t = Transmitter Power
G_t = Transmitter Antenna Gain
A_e = Effective Aperture of Receiver
$A_e = k \pi r^2$
$k = 0.55$
r = Radius of Antenna (20 ft)
S = Slant Range = 11,000 feet

such that

$$P_r = \frac{P_t G_t kr^2}{4S^2}$$

TABLE I

2 r = 40' Dish Electrical Characteristics

Frequency (MHz)	Gain (db)	E-Plane .5PBW	H-Plane .5PBW
300	29	6.0^o	5.4^o
600	35	3.0^o	2.7^o
900	38.5	2.0^o	1.8^o
1200	41.2	1.5^o	1.3^o
1500	43.0	1.2^o	1.1^o

TABLE II

ARC-27 Spurious Emissions (f_o = 312.5 MHz)

S.N. 1167			S.N. 3410			S.N. 4589		
Freq.	Pwr. (dbm)	Pwr. (watts)	Freq.	Pwr. (dbm)	Pwr. (watts)	Freq.	Pwr. (dbm)	Pwr. (watts)
f_o	+42.0	15.85	f_o	+37.5	5.5	f_o	+40.0	10.0
$2f_o$	+13.0	.02	$2f_o$	+15.0	.031	$2f_o$	+15.0	.031
$3f_o$	-3.0	.0004	$3f_o$	-3.0	.0005	$3f_o$	-2.5	.0006
$4f_o$	-7.0	.0002	$4f_o$	-6.5	.0002	$4f_o$	-10.0	..0001
$5f_o$	-2.5	.0006	$5f_o$	-10.0	.0001	$5f_o$	-20.0	.00001

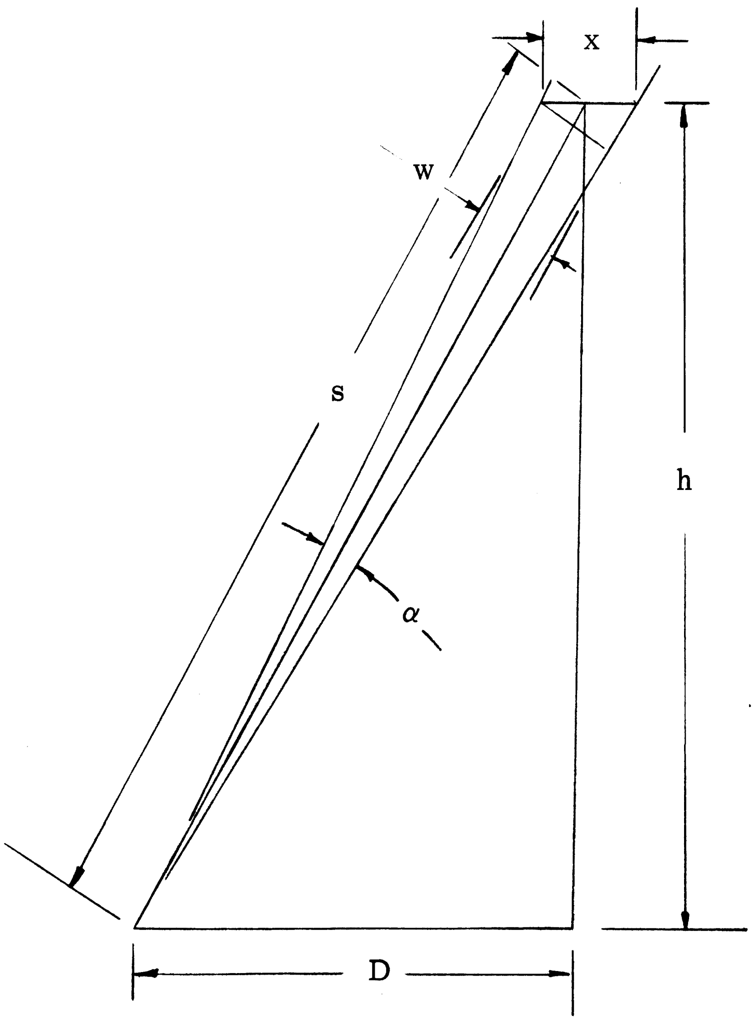

$$S = (h^2 + D^2)^{1/2} \doteq 11\,(10)^3$$

where $h = 10,000$ feet

$D = 5,280$ feet

$$w = S\,\alpha \doteq 230 \text{ feet}$$

where $\alpha \doteq 1.2^{\circ}$

$$x = \frac{w}{\cos 30^{\circ}} \doteq 265 \text{ feet}$$

FIG. 1: Geometry of Problem

and

$$P_r\,(\text{db}) = P_t\,(\text{db}) + G_t\,(\text{db}) + 20\log R - (6\,\text{db} + 20\log S)$$

$$= \left[P_t\,(\text{db}) + G_t\,(\text{db}) \right] - 66\,\text{db}$$

To obtain the directivity of the transmitting antenna use has been made of three dimensional pattern data for the modified monopole mounted on a simplified model of the T-33 aircraft. The gain of the modified monopole was obtained by reducing its directivity by the appropriate missmatch (VSWR) loss factor. The VSWR data was collected with the modified monopole over a 4 foot circular ground plane. The directivity, VSWR and gain data are shown in Table III.

From the geometry of the problem shown in Fig. 1, it can be deduced that the pattern recorded during the fly-by tests will be a conical pattern. The included half angle will be 30^o as measured from the normal to the underside of the aircraft. Therefore, it has been necessary to modify the transmitting antenna gain figure to account for this 30^o angle. To obtain a more realistic transmitted power level, the data of Table II was averaged. The transmitter power level and antenna gain are noted in Table IV along with the probable power received. The last column of Table IV denotes the margin of safety between the receiver sensitivity (-87 dbm) and the actual power available at the output terminals of the 40 foot reflector. From Table IV it can be seen that at the fundamental frequency there will be approximately a 58 db margin of safety between the receiver sensitivity and the power available at

TABLE III

Modified Monopole Electrical Characteristics (f_o = 300 MHz)

Frequency	VSWR	Directivity	Gain (G_t)
f_o	2.6:1	6.1 db	5.2 db
f_2	1.8:1	7.6 db	7.1 db
f_3	5.0:1	6.5 db	4.0 db
f_4	7.0:1	6.1 db	2.6 db
f_5	10.0:1	7.5 db	3.0 db

TABLE IV

Predicted Power Received (30^o From Normal to Aircraft)

$$P_r = (P_t + G_t) - 66 \text{ db}$$

Frequency	P_t (dbm)	G_t (db)	P_r (dbm)	ΔP_r (dbm)
f_o	40	-3	-29	58.0
f_2	14	-3.5	-55.5	31.5
f_3	-3	-0.3	-69.3	17.7
f_4	-8	1.3	-72.7	14.3
f_5	-18	2.0	-82	5.0

the output of the 40 foot reflector. However, for the second through fifth harmonics, the power level will be but a few db above the minimum detectable signal of the receiver. Since it will be desirable to record patterns both at the fundamental and harmonic frequencies, it will be advantageous to use a more sensitive receiver such that a greater dynamic range will be possible at the harmonic frequencies.

To ensure that the receiving system has an adequate dynamic range so that a sufficient amount of useful data will be collected, two RFI receivers will be required to collect data at the fundamental and second harmonic frequencies. In addition to the two RFI receivers, a Wide Range High Sensitivity Receiver is recommended for obtaining data at the third or fourth harmonic frequency of the AN/ARC-27 transmitter. Wide Range High Sensitivity Receivers typically have a sensitivity of -100 dbm such that a safety factor of 31 - 43 db would be available at the higher harmonics.

In the above discussion, it has been assumed that the antenna on the aircraft will be flying directly through the pattern maximum of the 40 foot reflector. However, this is not probable since the RF window through which the aircraft must fly will be approximately 230 by 265 feet as may be concluded from Fig. 1. Further, we have assumed that the radiation pattern of the 40 foot reflector is triangularly shaped (polar coordinates), which if true (as we know it is not), the aircraft would have to be flown precisely along the plotted course to insure that it would pass through the radiation pattern of the 40 foot reflector each time it passed over the ground reference point. An additional limitation is that the aircraft will be within the RF window (of the 40 foot reflector) for less than a second if we assume it is being flown 250 mph (360 feet per second). Since the radiation characteristics of the 40 foot reflector are not triangularly shaped but rather have a parabolic configuration, the RF window may be larger. For example, assuming the 10 db beamwidths (rather than the 3 db beamwidths of Table I) the aircraft will be within the RF window for approximately 3 seconds which would be more desirable.

Because of the limitations associated with using the Trebein facilities consideration was next given to the use of the Rome Air Development (RADC) facilities.

2.1.2 <u>Fly-By Tests RADC</u>

Three techniques are employed at the Rome Air Development Center (RADC) to obtain antenna patterns from an airborne antenna. The technique used normally is similar to that outlined in the Final Report prepared under Contract AF 33(615)-1964. It will be recalled in the above report a reference point was located on the ground and the aircraft flown over it from several points of the compass and pattern data obtained on a point-by-point basis. A second technique employed by RADC also employs a ground reference point to have an aircraft flown across the point tangentially to it such that data is collected continuously as the aircraft flies past. Sufficient data is collected so that the pattern may be reconstructed. The third technique also requires a reference point on the ground. The aircraft is flown along a radial that extends from the ground test site through the ground reference point. Data is collected continuously as the aircraft is flown from several miles away from the ground test site directly overhead to several miles in the opposite direction from the test site and reference point.

The principal difference between the technique employed by RADC and that noted in the Final Report of AF33(615)-1964 is that RADC uses a radar system to continuously track the aircraft. An antenna pedestal is slaved to the radar tracking antenna such that the pedestal follows the movement of the radar antenna in both azimuth and elevation. Receiving antennas are mounted to the slaved antenna pedestal and track the aircraft such that data is collected continuously. Up to 8 antennas may be mounted on the pedestal at one time. However, for the purposes of our tests only 3 antennas will be required. The frequency range of this system is 100 MHz to 10 GHz.

The radar system used is an MSQ auto tracker which has better than 1^o accuracy. A second system that may be used is an MSQ 63, which is operational in the frequency range of 250 MHz to 40 GHz. However, when using this system it is not possible to track the aircraft (with radar) as it is using the MSQ auto tracker and, therefore, the accuracy would be less.

Presently two KC-135 aircraft are instrumented to obtain radiation patterns of airborne antennas, and two C-131 aircraft are instrumented to obtain radiation patterns of ground based radar systems. For the present task, only one of the KC-135 aircraft would be required. The KC-135 is a Military version of the commercial Boeing 707. Each of the KC-135's used by Rome has from 30 to 40 antennas mounted on the underside of the fuselage.

The system employed to obtain antenna patterns using an instrumented aircraft requires three facilities: 1) the airborne, 2) radar, and 3) the receiving facility. The three facilities are inter-connected through radio communications to facilitate communicating between them. The procedure is for the radar system to track the aircraft and to provide ground control to ensure the aircraft is flown over the point of interest. The receiving system monitors the data as the aircraft approaches the point and if the reference point is missed by too great a distance, the operator may request the aircraft to be flown over the data point again at the completion of that test flight. The test procedure requires that the aircraft be flown over the point of interest a sufficient number of times to obtain 24 data points (15^{o} increments).

At the present time RADC has selected three points on the ground as reference points. These points have been chosen so that omnidirectional patterns may be recorded at elevation angles of 5^{o}, 8^{o} and 12^{o} below the local horizon of the aircraft. The aircraft is generally flown at an altitude of 35,000 feet, such that the ground reference points are several miles from the test site. Typically the aircraft can be flown within 500 feet of the selected ground point which is considered to be adequate for obtaining antenna patterns from an instrumented aircraft.

To obtain a single antenna pattern (employing the KC-135) would require approximately five hours of flight time. Therefore, to obtain the data required for the simplified modeling study, a conservative estimate of 50 to 100 hours of flight time would be required.

III. DATA RECORDING AND REDUCTION TECHNIQUES

In the previous interim, it was recommended that a technical report be prepared on the data handling techniques developed by Michigan. Preliminary work on this report is progressing and it is anticipated that the report will be completed prior to the conclusion of the present contract. No significant changes have been made since the writing of the previous interim and therefore no further discussion will be given at this time.

IV. A SYSTEM ASPECT

The system study is being continued, employing the AN/ARC-27 transmitter. Additional spectrum signature data has been collected employing both a Polarad and a Hewlett-Packard spectrum analyzer as well as two Empire Device RFI meters. Three sets of data have been obtained using these instruments. It is, however, difficult to correlate the results at the present time.

Additional studies have been conducted to determine the output impedance of the transmitter. Approaches being considered are Reiche diagrams, cold tests and techniques for measuring the absolute output impedance of the transmitter.

4.1 Source Impedance Measurement

In the first interim report, the power transfer from a transmitter to an antenna was shown to require measurement of the internal impedance of the transmitter. Here it will be shown that, if the transmitter impedance is not a function of the termination, the impedance can be measured with a line stretcher terminated in a short circuit and a detector tuned to the frequency of interest. The measurement procedure is very similar to that for measuring a termination impedance with a slotted line.

The circuit used is shown schematically in Fig. 2. The transmitter is represented by a voltage source E_s and a series impedance Z_s.

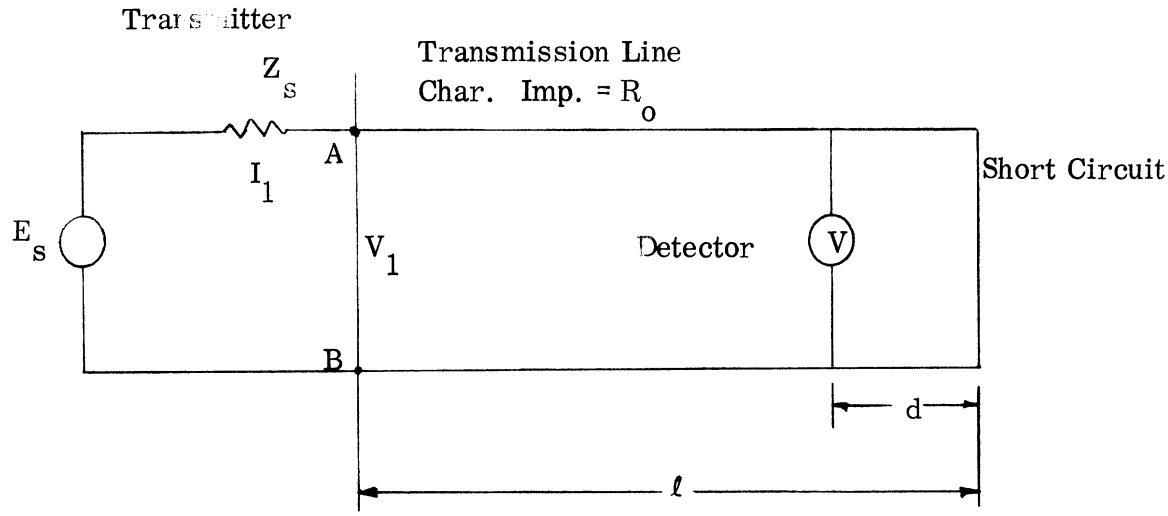

FIG. 2: Measurement Circuit

Neither E_s nor Z_s are a function of the termination. The transmitter terminals AB are connected to a transmission line of variable length, ℓ. A detector, tuned to the frequency of interest, is placed across the line a fixed distance, d, from the short circuit. The exact value of d is not important but should remain fixed throughout a measurement. The largest voltage for the detector is obtained when $d \doteq \lambda/4$, $3\lambda/4$, etc, but the effect of detector loading is most pronounced at these points. For a measurement device, $d \doteq \lambda/8$ may be a good compromise.

The impedance Z_t seen at the input of a shorted transmission line of length ℓ and propagation constant k is given by:

$$Z_t = jX_t = jR_o \tan k\ell \qquad (1)$$

This is the impedance seen looking to the right of terminals AB of Fig. 6. The voltage V_1 across terminals AB is given by:

$$V_1 = |I_1 jX_t| \tag{2}$$

$$= \frac{E_s |X_t|}{|Z_s + jX_t|} \tag{3}$$

let $Z_s = R_s + jX_s$ (4)

then

$$V_1 = \frac{E_s |X_t|}{\sqrt{R_s^2 + (X_s + X_t)^2}} \tag{5}$$

$$= \frac{E_s R_o |\tan k\ell|}{\sqrt{R_s^2 + (X_s + R_o \tan k\ell)^2}} \tag{6}$$

Because the transmission line is shorted at the far end, an infinite sinusoidal standing wave appears on the line such that

$$V_1 = V_p (\sin k\ell) \tag{7}$$

The quantity V_p represents the peak value of the standing wave appearing at every odd number of quarter wavelengths from the short. The voltage, V, indicated by the detector will be some fixed fraction, a, of this peak voltage. Hence,

$$V = aV_p \tag{8}$$

Combining equations 6, 7, and 8, we obtain

$$V \frac{|\sin k\ell|}{a} = \frac{E_s R_o \left|\tan k\ell\right|}{\sqrt{R_s^2 + (X_s + R_o \tan k\ell)^2}} \tag{9}$$

from which

$$V = \frac{a E_s}{\sqrt{\left[\frac{R_s}{R_o}\right]^2 \cos^2 k\ell + (\frac{X_s}{R_o} \cos k\ell + \sin k\ell)^2}} \tag{10}$$

In equation 10, the magnitude signs are no longer necessary; the positive sign is attached to the radical in the denominator.

Now let us examine equation 10 for the condition of $R_s = R_o$ and $X_s = 0$. Equation 10 becomes

$$V\Big|_{\substack{R_s = R_o \\ X_s = 0}} = \frac{a E_s}{\sqrt{\cos^2 k\ell + \sin^2 k\ell}} \tag{11}$$

$$= a E_s \tag{12}$$

Thus when the source impedance matches the line impedance ($Z_s = R_o$) the detector reading is independent of the line length ℓ. This condition is equivalent to the matched termination of a line that produces a flat line. The flat line counterpart for a "source standing wave" is demonstrated by equation 12.

Now what happens when $Z_s \neq R_o$, i.e., the source impedance is not matched. For this situation, let us consider, in general, the situation viewed at terminals AB but at terminals A'B' a distance ℓ_1 from the transmitter. Let us choose ℓ_1 such that the transmitter impedance Z_s is transformed to a pure resistance R'_s so that $R'_s \geq R_o$. Equation 10 then becomes

$$V = \frac{a E'_s}{\sqrt{\left[\frac{R'_s}{R_o}\right]^2 \cos^2 k(\ell - \ell_1) k + \sin^2 k(\ell - \ell_1)}} \tag{13}$$

Equation 13 has a maximum value when $\cos k(\ell - \ell_1) - 0$ and a minimum value when $\sin k(\ell - \ell_1) = 0$. To show this, differentiate the quantity under the radical and set it equal to zero.

$$\frac{d}{d\left[k(\ell - \ell_1)\right]}\left[\left[\frac{R'_s}{R_o}\right]^2 \cos^2 k(\ell - \ell_1) + \sin^2 k(\ell - \ell_1)\right]$$

$$= -2\left[\frac{R'_s}{R_o}\right]^2 \sin k(\ell - \ell_1) \cos k(\ell - \ell_1) + 2 \sin k(\ell - \ell_1) \cos k(\ell - \ell_1) \tag{14}$$

$$= 2\left[1 - \left[\frac{R'_s}{R_o}\right]^2\right] \sin k(\ell - \ell_1) \cos k(\ell - \ell_1) \tag{15}$$

Equation 15 is zero when

$$\sin k(\ell - \ell_1) = 0 \tag{16}$$

or

$$\cos k(\ell - \ell_1) = 0 \tag{17}$$

Using equation 16 in 13 we have

$$V_{min} = a E'_s \frac{R_o}{R'_s} \tag{18}$$

Using equation 17 in 13, we have

$$V_{max} = a E'_s \tag{19}$$

Equation 18 gives V_{min} because $R'_s < R_o$.

Now, dividing equation 18 by equation 19 gives

$$\frac{V_{max}}{V_{min}} = \frac{R'_s}{R_o} \tag{20}$$

To determine the impedance seen looking back into the transmitter terminals AB, we must enter the Smith Chart at

$$\frac{R'_s}{R_o} = \frac{V_{max}}{V_{min}} = \text{VSWR}$$

and go around the chart a distance equivalent to ℓ_1 in the direction "toward the load" indicated on the chart. This point on the chart represents the transmitter impedance Z_s.

4.2 Complex Impedance Load

In the previous section it was assumed that the transmitter impedance was not a function of the load. In this section consideration will be given to techniques for fabricating a laboratory load whose impedance is matched to the transmission line at f_o and unmatched at harmonics of f_o.

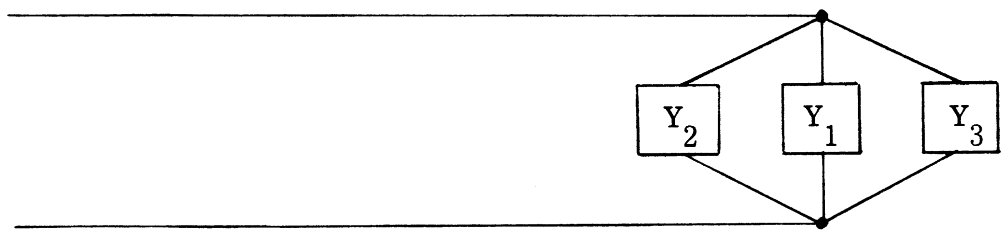

FIG. 3: Circuit for Terminating a Coaxial Line

Let Y_1 be matched to the characteristic admittance, G_o, of the line, i.e.,

$$Y_1 = G_o. \tag{21}$$

Now, if at the fundamental frequency

$$Y_2 = -Y_3 \tag{22}$$

the termination of the line is

$$Y_t = Y_1 + Y_2 + Y_3 \tag{23}$$

$$= Y_1 = G_o \tag{24}$$

Now what is the condition that satisfies equation 22? If Y_2 and Y_3 are obtained from shorted transmission lines of lengths ℓ_2 and ℓ_3 respectively, then

$$Y_2 = jG_o \tan k\ell_2 \tag{25}$$

$$Y_3 = jG_o \tan k\ell_3 \tag{26}$$

Hence, to satisfy equation 22

$$j G_o \tan k\ell_2 = -jG_o \tan k\ell_3 \tag{27}$$

or

$$\tan k\ell_2 = -\tan k\ell_3 \tag{28}$$

From trigonometry,

$$\tan A = -\tan(\pi - A); \quad \text{if } 0 < A \leq \pi \tag{29}$$

Hence

$$\tan k\ell_2 = \tan(\pi - k\ell_2) \tag{30}$$

or

$$k\ell_2 = \pi - k\ell_3 \tag{31}$$

from which

$$\ell_2 + \ell_3 = \frac{\pi}{k} = \frac{\lambda}{2} \tag{32}$$

At the desired harmonic frequency, either ℓ_2 or ℓ_3 (or both) must be one half wavelength long for the load conductance at the junction Y_1 to be effectively short circuited. Since equation 32 shows that either length ℓ_2 or ℓ_3 can be arbitrarily chosen, let ℓ_2 be assigned a value $(a\lambda)/2$ at the desired harmonic frequency. If a is an integer $0 < a < n$, then ℓ_2 will short circuit Y_1. Thus

$$\ell_2 = \frac{a\lambda_n}{2} \qquad (33)$$

in which $n = 2, 3, 4, \ldots$ as desired.

Since

$$\lambda_n = \frac{a\lambda}{n} \qquad (34)$$

equation 32 becomes

$$\ell_2 = \frac{a\lambda}{2n} \qquad (35)$$

and

$$\ell_3 = \frac{(n-a)\lambda}{2n} \qquad (36)$$

Figure 4 illustrates one technique for constructing this load.

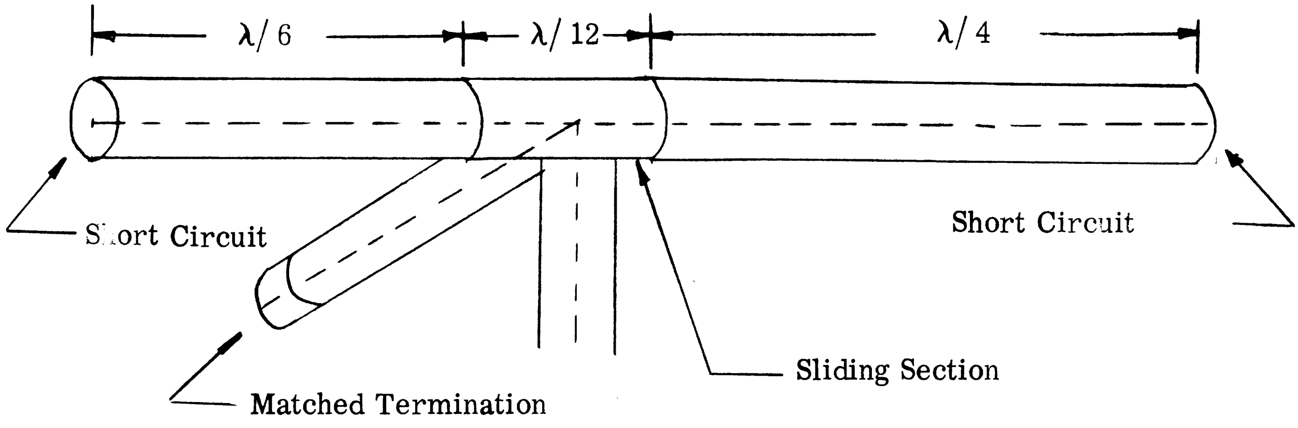

FIG. 4: Load Construction

The sliding section need slide only $\lambda/12$ to the left of the center of the shorted section. In operation, the sliding section would be adjusted to satisfy equations 35 and 36 at the harmonic frequency of interest.

An alternate load is shown in Fig. 5.

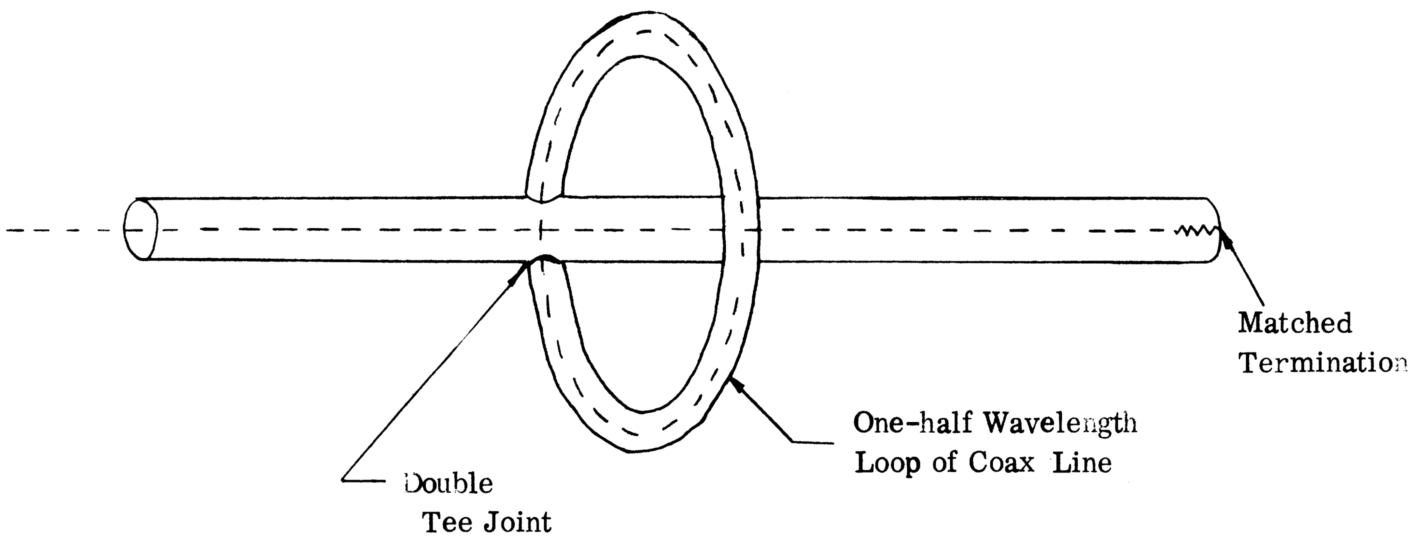

FIG. 5: Alternate Load

The load of Fig. 5 has not been analyzed thoroughly, but appears to be automatically adjusted for all harmonic frequencies. It has two advantages over the construction of Fig. 4. First, no adjustment is necessary for the various harmonics, and second the load is easily changed (by replacing the half wavelength loop) to another fundamental frequency.

4.3 AN/ARC-27 Study

The purpose of the investigation was to scan the spectrum, locate, measure and record the spurious emissions of the transmitter under test. The measurements were performed as a closed-system test, i.e., the output power from the transmitter was fed to a medium power, 50 ohm dummy load. A signal sampler (directional coupler) was used to couple a small portion of the output to a rf receiver. Four rf receivers were employed during the testing.

Initially, a Polarad Spectrum Analyzer, Model TSA-S, was employed as the receiver in the test set-up as shown in Fig. 5. The transmitter was tuned to a fundamental frequency f_o = 300 MHz for this test and all subsequent tests. The spectrum was scanned by the analyzer from 10 - 1500 MHz. This frequency range was chosen so as to encompass all emissions up to and including the fifth harmonic spurious emission. The signals observed on the spectrum analyzer are listed in Table V. It is to be emphasized that the only signals that appeared on the analyzer that were felt to have their origin in the transmitter output were the fundamental and harmonic frequency emissions. The origin of all the other "apparent" signals listed in the table (referred to as "unreal") can be shown to be due to the spectrum analyzer, i.e., spurious responses of the measuring equipment itself. It is to be noted that these "unreal" responses were not image signals. Their generation within the analyzer might have been prevented by the insertion of appropriate frequency rejection networks or filters ahead of the analyzer, but these devices were

TABLE V

Spurious Frequency		Origin of Signal
Lower Dial	Upper Dial	
71.0	-	Unreal
78.0	-	Unreal
94.5	350	Unreal (Both)*
106	372	Unreal (Both)
118	396	Unreal (Both)
174	509	Unreal (Both)
197	555	Unreal (Both)
224	606	$606 = 2 f_o$
259	678	Unreal (Both)
303	765	$303 = f_o$
375	909	$909 = 3 f_o$
398	955	Unreal (Both)
965	2090	Unreal (Both)
1114	2386	Unreal (Both)
1193	2548	$1193 = 4 f_o$
1375	2910	Unreal (Both)
1388	2938	Unreal (Both)
1414	2988	Unreal (Both)
1449	3055	Unreal (Both)
1475	3110	Unreal (Both)
1490	3140	$1490 = 5 f_o$

* Either the upper or lower dial reading gives correct frequency. Determination of frequency of "unreal" signals not shown.

not immediately available. Also, since there appeared to be no convenient means for measuring the relative power level of signals observed on the Polarad Analyzer, no results are given. It is therefore recommended that the above spectrum analyzer not be used for spurious emission measurements unless appropriate filters are available and the results are viewed with some suspicion.

A second test was conducted with the measurement set-up shown in Fig. 5, but with a Hewlett-Packard Spectrum Analyzer, Model 851A/8551A, used as the receiver. The frequency range scanned was again 10 - 1500 MHz, with the transmitter again tuned to 300 MHz. The results of this test, shown in Table VI, indicated the presence of two non-harmonic spurious emissions at frequencies of 160 and 660 MHz in addition to the fundamental and four harmonic emissions. The relative power level of the signals observed on the analyzer were recorded and referenced to the fundamental signal. The fundamental power output was determined absolutely by means of a power meter. The coupling factor of the signal sampler and the insertion loss of the fixed attenuators were assumed flat across the frequency range of interest. It is felt the Hewlett-Packard Spectrum Analyzer yielded a convenient, first-order approximation of the spectrum produced by the transmitter.

The final spurious emission measurements were conducted with more refined measuring equipment and a test set-up as shown in Fig. 6. The test procedure followed that outlined in section 5.2.3.3 of MIL-STD-449 B. Two frequency

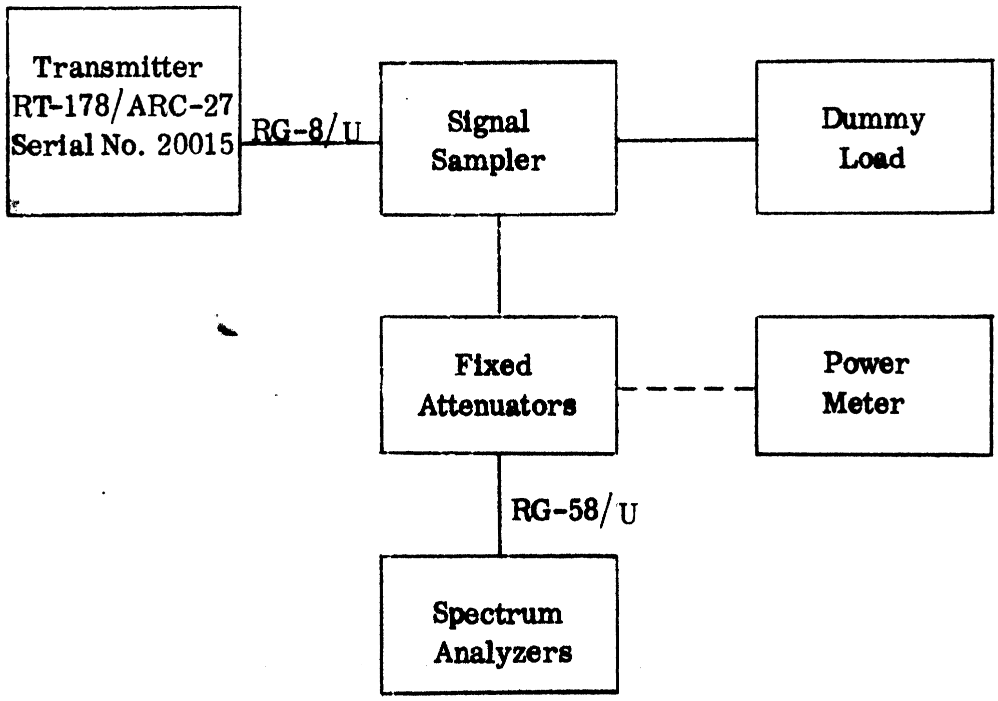

FIG. 5: **Initial Spurious Emission Measurement Block Diagram**

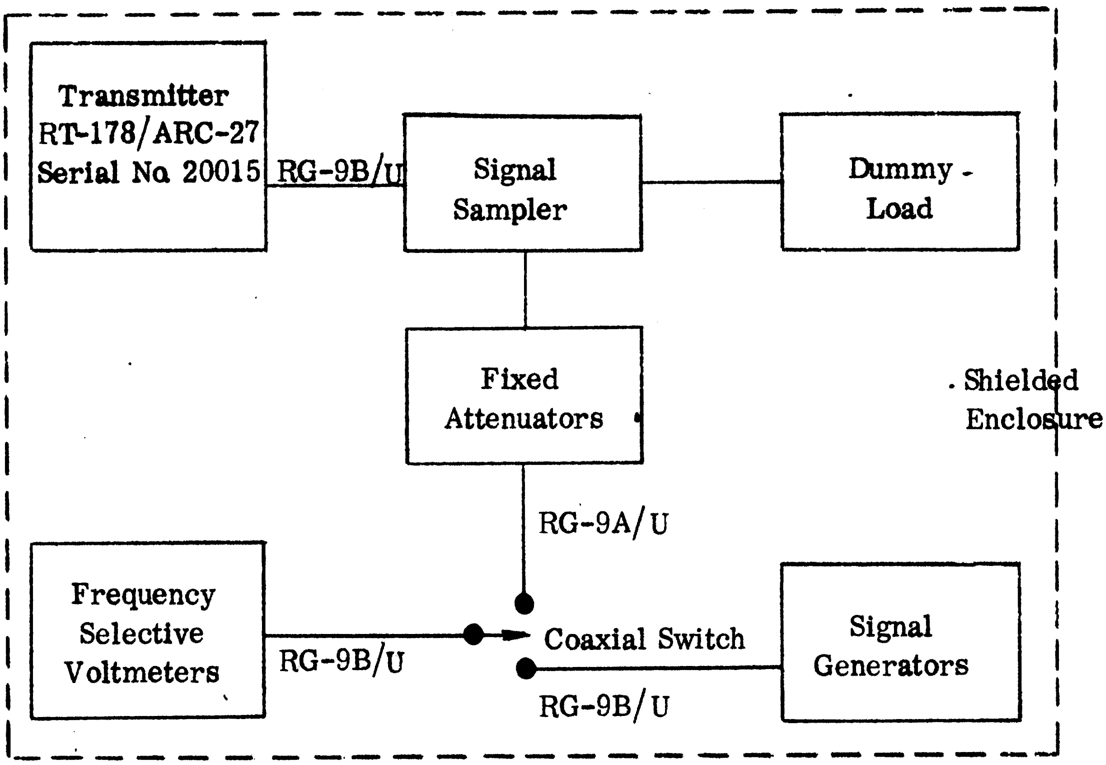

FIG. 6: **Final Spurious Emission Measurement Block Diagram**

TABLE VI

Spurious Frequency (MHz)	Origin of Signal	Spurious Power Output (Average) (dbm)
160		-12.0
300	f_o	+44.0
600	$2f_o$	+17.0
660		-8.0
900	$3f_o$	-10.0
1200	$4f_o$	-8.0
1500	$5f_o$	+12.0

selective voltmeters, Empire Devices Models NF-105 and NF-112, were employed as rf receivers. The results obtained with these high sensitivity meters are shown in part in Table VII. The table lists the significant spurious emissions observed between 300 and 1500 MHz, namely, four harmonic emissions and one non-harmonic emission at 658 MHz. The power output of each spurious signal was determined by duplicating the voltmeter response to the spurious signal with a signal generator substituted for the transmitter. The power output was then given by the sum of the signal generator output dial reading in dbm and the signal sampler coupling factor and attenuator insertion loss in db at the frequency of interest.

Also shown in Table VII is a selected group of low power spurious emissions from 240.0 to 285.0 MHz. This group is representative of the transmitter emission spectra that appeared to exist over much of the frequency range scanned, i.e., 20 - 1500 MHz. It is not felt that the insertion of a fundamental frequency rejection network would alter the results as shown. The entire frequency range was not scanned for the low-level emissions due to a limitation of testing time and the lack of certainty as to the importance of these signals. It was evident, however, that if the importance of the low-level emissions is established, a more thorough investigation with frequency selective voltmeters will be required to determine the exact nature of the transmitter spectrum.

TABLE VII

Spurious Frequency (MHz)	Origin of Signal	Attenuation Inserted (db)	Signal Generator (dbm)	Spurious Power Output (Average) (dbm)
240.0		20	-35.0	-15
255.0		20	-53.0	-33
260.0		20	-59.0	-39
278.0		20	-74.0	-54
280.0		20	-60.0	-40
285.0		20	-53.0	-33
———	———	———	———	———
300.0	f_o	50.0	-5.0	+45.0
600.0	$2f_o$	21.0	-10.0	+11.0
658.0		21.0	-55.0	-34.0
900.0	$3f_o$	20.0	-17.5	+2.5
1200.0	$4f_o$	20.5	-29.0	-8.5
1500.0	$5f_o$	20.5	-15.0	+5.5